

# Enrichment of Coal-Bed Methane by PSA Complemented with CO<sub>2</sub> Displacement

Congmin Liu and Yaping Zhou

Dept. of Chemistry, School of Science, Tianjin University, Tianjin 300072, China

Yan Sun, Wei Su, and Li Zhou

High Pressure Adsorption Laboratory, School of Chemical Engineering and Technology, Tianjin University, Tianjin 300072, China

DOI 10.1002/aic.12305

Published online July 13, 2010 in Wiley Online Library (wileyonlinelibrary.com).

*A PSA cycle complemented with CO<sub>2</sub> displacement was studied for enriching coal-bed methane (CBM). The column was first pressurized to the adsorption pressure with feed gas, and then N<sub>2</sub> was produced at column top in step 2. The feed gas switched to CO<sub>2</sub> at the end of step 2, and the adsorbed CH<sub>4</sub> was displaced and pushed to column top by CO<sub>2</sub> becoming the second column-top product in step 3. The CO<sub>2</sub> stream was shut off before it broke through the sorption bed. Then bed regeneration followed. A series of CH<sub>4</sub>/N<sub>2</sub> mixtures containing 17.62 to 51.33% CH<sub>4</sub> was used for feed gas. It was experimentally shown that the product concentration was higher than 90%, and methane recovery was higher than 98% even for the feed of low-methane concentration. Displacement at ambient pressure was shown more efficient than the displacement at adsorption pressure for the enrichment. © 2010 American Institute of Chemical Engineers AICHE J, 57: 645–654, 2011*

**Keywords:** separation, coal bed methane, enrichment, PSA, CO<sub>2</sub> displacement

## Introduction

Coal bed methane (CBM) is a kind of natural gas formed geologically or biologically in coal seams. The world's CBM resource buried in the top 2000 m of the earth is up to  $2.4 \times 10^{15}$  m<sup>3</sup>, which is more than two times that buried in natural gas reservoirs.<sup>1</sup> Most CBM has not yet been exploited. High-quality CBM may serve as chemical raw stock or clean fuel; however, the poor quality CBM always is released to the atmosphere, which is hazardous to the environment because the greenhouse effect of CH<sub>4</sub> is 21 times higher than CO<sub>2</sub>.<sup>2</sup> In order to serve as chemical raw stock, the CH<sub>4</sub> content in CBM must be higher than 80%, and higher than 90% in order to merge in the pipeline network of civil natural gas.<sup>3</sup> However, methane concentration

in the usual seam drainage gas is in the range of 20–45%. The other constituents are mainly incombustible N<sub>2</sub> and CO<sub>2</sub>. Therefore, the key problem for the utilization of CBM is the enrichment of CH<sub>4</sub> from its mixture with N<sub>2</sub> and CO<sub>2</sub>. CO<sub>2</sub> may or may not exist in CBM, and the difference between CH<sub>4</sub> and CO<sub>2</sub> in separation is larger than that between CH<sub>4</sub> and N<sub>2</sub>; therefore, the pair of key components for the enrichment is CH<sub>4</sub>/N<sub>2</sub>. Separation of CH<sub>4</sub>/N<sub>2</sub> was considered as a challenge due to the similarity of the two gases in physicochemical properties.<sup>4</sup> Cryogenic distillation, membrane and PSA (pressure swing adsorption) are considered as the major technologies applicable for the separation presently. The cryogenic method may be applied for large-scale production since a huge investment and large-energy consumption are involved.<sup>5</sup> Membrane separation is a hot topic of research; however, there is still a distance to industrial application due to the poor selectivity and unsatisfactory working life of available membranes.<sup>6,7</sup> PSA is also a young separation technology since it did not appear in industry

Correspondence concerning this article should be addressed to L. Zhou at zhouli@tju.edu.cn.

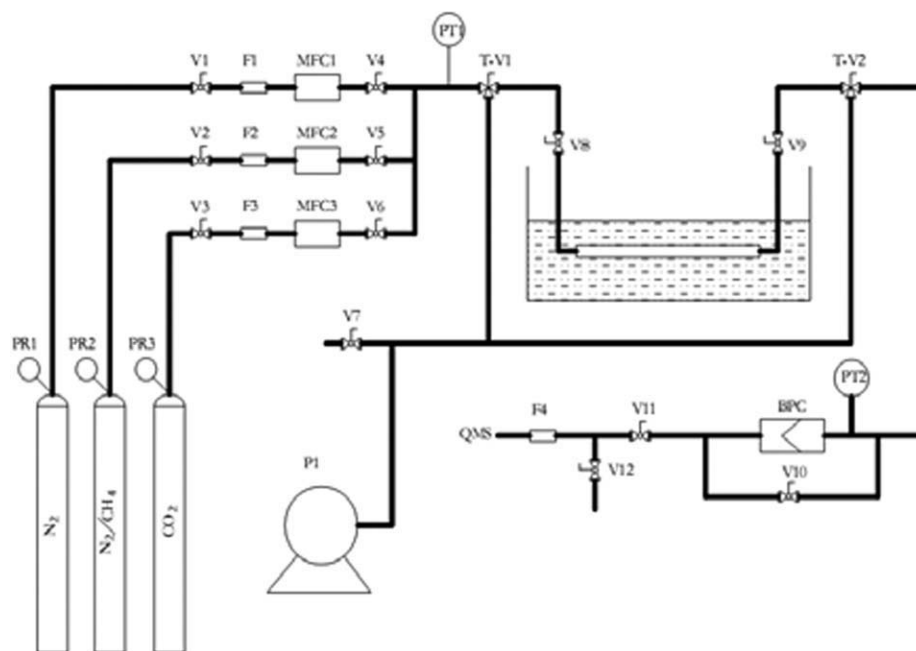


**Chart 1. Flow chart of experimental setup.**

Pressure regulator (PR), filter (F), valve (V), three-way valve (T-V), mass-flow controller (MFC), pressure transducer (PT), backpressure controller (BPC), pick-up pump (P1), and quadrupole mass spectrograph (QMS).

until the 1970s. However, it has been extensively used in petroleum, chemical and petrochemical or air separation industries in the following years. It operates at ambient temperature and a reasonable pressure. The equipment is simple and highly automated with large flexibility of operation. Investment in adsorbents may be large; however, the working life of adsorbents is usually long. Therefore, PSA attracts extensive interest for the separation of industrial gases due to the advantage of low cost and energy effectiveness.<sup>4,8,9</sup>

Many adsorbents have been tested for the  $\text{CH}_4/\text{N}_2$  separation. If the separation is based on the difference of components at equilibrium adsorption, activated carbon was usually applied.<sup>10</sup> Yang and coworkers reached a selectivity ratio of 4.25 by grafting  $\text{MoO}_2$  on high-surface carbon; however, the selectivity ratio decreased with pressure, and leveled off to about 3 at 12 atm.<sup>11</sup> Olajosy and coworkers used activated carbon in a VPSA process and enriched methane from 55.2% to 96–98%.<sup>12</sup> A simulation study showed that lower-adsorption pressure was preferred for the PSA separation between  $\text{CH}_4$  and  $\text{N}_2$ .<sup>13</sup> Methane is always adsorbed more strongly than nitrogen at equilibrium; therefore, it cannot be obtained at column top as long as the separation is based on the difference of equilibrium adsorption. As a bottom-product, both concentration and recovery of methane are limited not to mention the loss of pressure. Fortunately the kinetic property difference of the two gases allows methane to be collected at column top<sup>14</sup> when carbon molecular sieves (CMS),<sup>15–17</sup> synthesized zeolites,<sup>18–21</sup> clinoptilolites and their modified species<sup>22–26</sup> are used as adsorbents. Because  $\text{N}_2$  shows more adsorption preference over these materials,  $\text{CH}_4$  is obtained at column top. It was shown for 4A zeolite that improvement was observed only at relatively low-temperature (253 K);<sup>20</sup> however, a product with higher than 90%  $\text{CH}_4$  was obtained at 273 K.<sup>21</sup> Yang and coworkers pub-

lished a series of CBM enrichment studies on using clinoptilolites and their modified species as adsorbents. The original clinoptilolites increased the methane content from 85% to 97.3%; however, methane recovery was only 53.2%. Other studies worked on ZSM-5, SAPOs, ETS-4,  $\beta$ -zeolite and silicalite,<sup>27–31</sup> did not reach satisfactory enrichment either. Although this kind of adsorbents can switch over the adsorption preference of methane and nitrogen, its potential for industrial application is not promising due to the nonideal selectivity and low-adsorption capacity. Activated carbon is actually most suitable for industrial enrichment of CBM. The disadvantage of using activated carbon in PSA processes is that methane cannot be the column-top product; however, as shown it is possible to switch methane to column top by complementing conventional PSA cycle with a step of  $\text{CO}_2$  displacement in this study. Compared to  $\text{CH}_4$ ,  $\text{CO}_2$  is more strongly adsorbed on activated carbon; therefore, it can displace the adsorbed methane and push it up to the column top. As a column-top product, the enriched coal-bed methane can reach higher concentration and recovery even for the CBM of low-methane content. In addition, the product stream maintains its mechanical energy and yields low-energy cost in succeeding transportation.

## Experimental

### Apparatus

The experimental study on the proposed PSA process addressing to CBM enrichment was carried out in a setup shown schematically in Chart 1. A stainless steel tube with dimension of 250 mm long and 10 mm i.d. was used for the adsorption column, and activated carbon of 40–60 mesh was packed in. A backpressure regulator controlled the

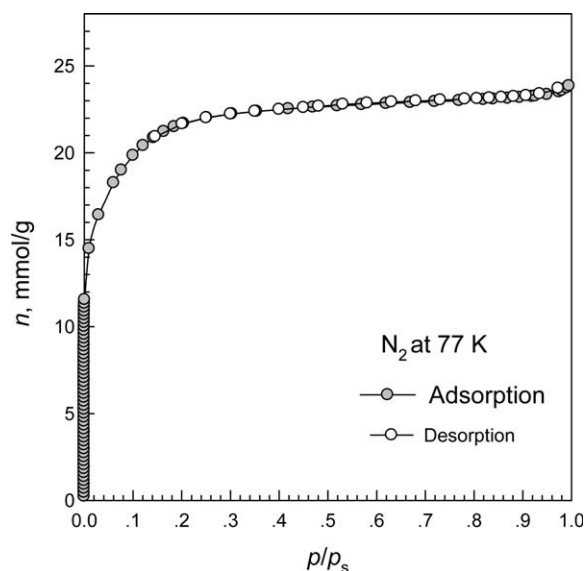


Figure 1. Adsorption/desorption isotherms of N<sub>2</sub> at 77 K.

adsorption pressure, and the pressure drop over the adsorption bed was set at 0.2 MPa. Pressure was measured and transmitted to a computer by pressure transmitters model SY-9411 provided by Advantech Co., Ltd. Beijing. The full measurement scale was 1 MPa with precision  $\pm 0.1\%$  F.S. The gas-flow rate was measured and controlled by mass flow controllers model SY-9312 provided by the same company. The full scale of measurement was 400 cm<sup>3</sup>/min of precision  $\pm 1.5\%$  F.S. Composition of the effluent stream was analyzed by a quadrupole mass spectrograph made in Stanford Research Systems, Inc. USA. All units were connected by stainless steel capillary tube of 2 mm i.d. and 0.5 mm wall thickness. The adsorption column was put in a thermostat with temperature constant to  $\pm 0.1$  K.

### Materials

The activated carbon used in the experiments was prepared in the authors' laboratory. A carbon sample was analyzed based on nitrogen adsorption and desorption isotherm at 77 K collected on Micromeritics ASAP 2020 and shown in Figure 1. The BET surface area, pore volume and the bed-packing parameters are shown in Table 1. The pore-size distribution determined by the DFT model<sup>32</sup> is shown in Figure 2. The activated carbon used in experiments is basically microporous as illustrated in Figures 1 and 2. The adsorption isotherms of CH<sub>4</sub>, N<sub>2</sub> and CO<sub>2</sub> on the carbon at 298 K were collected on a volumetric apparatus and shown in Figure 3. Details of the measurement were previously described.<sup>33</sup> The adsorbed amount of CO<sub>2</sub> was much higher than

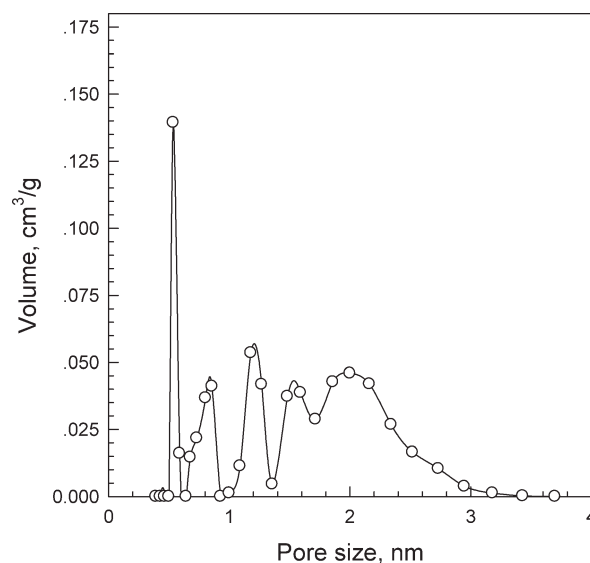


Figure 2. Pore-size distribution of carbon sample.

that of CH<sub>4</sub> and N<sub>2</sub>. The breakthrough curves of gas mixture He/CH<sub>4</sub>/N<sub>2</sub> were also collected at 298 K and shown in Figure 4. A separation coefficient between CH<sub>4</sub> and N<sub>2</sub> was determined as 3.5 based on the breakthrough curves. Details of the breakthrough experiment and calculation of the separation coefficient were described in the literature.<sup>26</sup> The carbon was dried *in vacuo* at 393 K for 8 h before experiments. All gases used in the experiments were provided by Liufang Gas Co. Tianjin. The purity of He and CH<sub>4</sub> is higher than 99.99%, and higher than 99.9% for N<sub>2</sub> and CO<sub>2</sub>. The composition of feed gases prepared for simulating real CBM is shown in Table 2.

### Procedure

The proposed PSA cycle was composed of four steps: pressurization, adsorption, CO<sub>2</sub> displacement, and regeneration. It

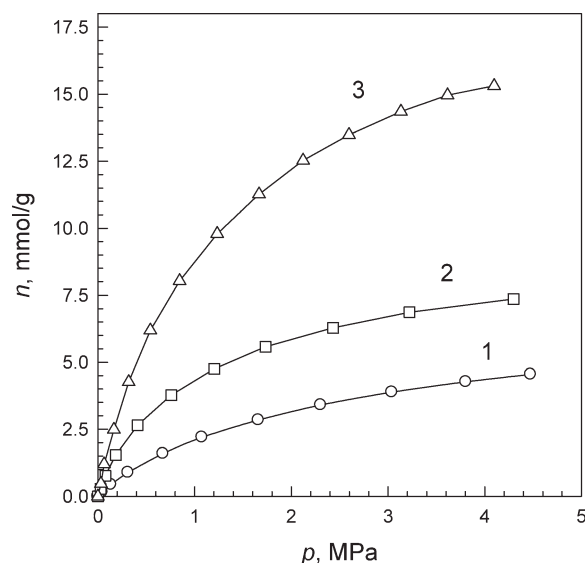
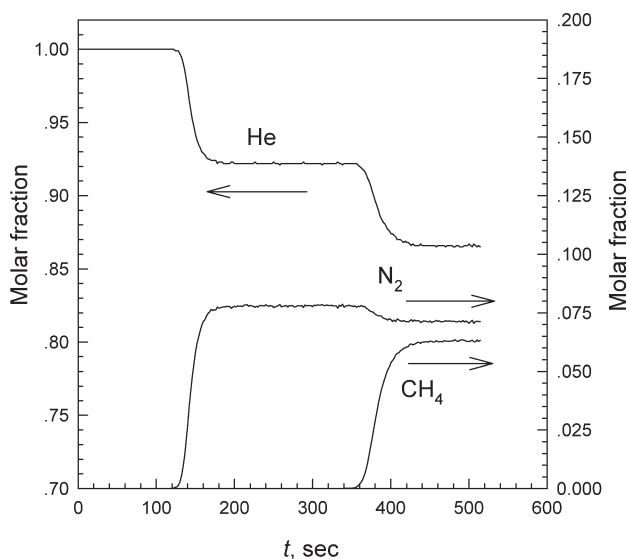


Figure 3. Adsorption isotherms of CH<sub>4</sub>, N<sub>2</sub> and CO<sub>2</sub> at 298 K.

(1) N<sub>2</sub>, (2) CH<sub>4</sub>, and (3) CO<sub>2</sub>.

Table 1. Carbon and Adsorption Bed Parameters

Parameter	Values
BET surface, m <sup>2</sup> /g	1700
Pore volume, cm <sup>3</sup> /g	0.83
Carbon weight in bed, g	7.29
Bulk density, g/cm <sup>3</sup>	1.94
Void space, $\epsilon$	0.77



**Figure 4. Breakthrough curves of the He/N<sub>2</sub>/CH<sub>4</sub> mixture passing the carbon bed at 298 K.**

featured inclusion of a CO<sub>2</sub> displacement step in a conventional PSA cycle. Compared to CO<sub>2</sub>, CH<sub>4</sub> became the weakly adsorbed component and was displaced and pushed up to the column top by CO<sub>2</sub>. The column pressure at each step is shown for a cycle in Figure 5. The column was first pressurized to the adsorption pressure (0.4 MPa) with feed gas in step 1. The feed gas continued to feed the column at the pressure, and pure N<sub>2</sub> was obtained at column top in step 2. The third step was CO<sub>2</sub> displacement; however, there are two modes of displacement. One mode was to switch the feed gas to CO<sub>2</sub> at the same pressure as adsorption. The CO<sub>2</sub> stream was shut off before it broke through the sorption bed, and the bed pressure was released concurrently to the ambient pressure at the end of step 3 as shown by branch 1 of Figure 5. Another mode was to release the bed pressure concurrently to ambient at the end of step 2, and then to allow CO<sub>2</sub> stream to feed the sorption bed at ambient pressure, and to shut off the CO<sub>2</sub> stream at the end of step 3 as shown by branch 2 of Figure 5. Two concentration profile borders, N<sub>2</sub>/CH<sub>4</sub> and CH<sub>4</sub>/CO<sub>2</sub>, were formed in the sorption bed during step 3 as shown in Chart 2 no matter which displacement mode was applied. Nitrogen was still the column top product in the early time of step 3; however, both borders moved toward the column top following the feeding of CO<sub>2</sub>, and methane became the second column top product of step 3 when the profile front of CH<sub>4</sub> broke through the bed. The sorption bed was saturated by CO<sub>2</sub> when the front of CO<sub>2</sub> profile reached bed top at the end of step 3; therefore, the fourth step was regeneration. Two regeneration methods were tested

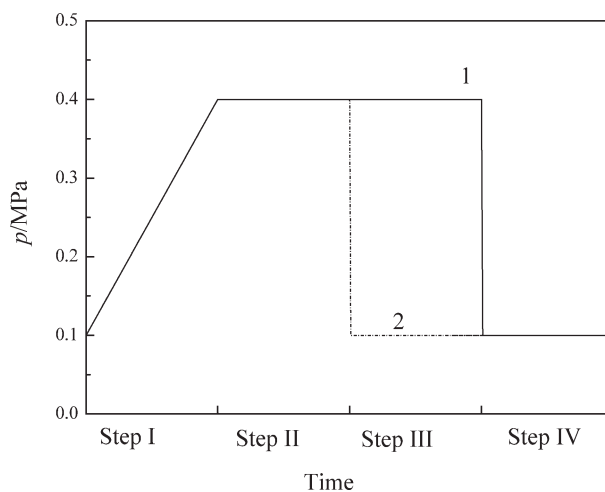


**Figure 5. Pressure histories of a cycle.**

(1) Displacement at 0.4 MPa, and (2) displacement at 0.1 MPa.

in experiments: purging by pure nitrogen previously obtained or by evacuation.

#### Performance evaluation

To evaluate the performance of the proposed PSA cycle, aside from product concentration, some other performance indices were defined. Methane recovery was defined as

$$\text{CH}_4 \text{ recovery} = \frac{V_{\text{out}} c_{\text{out}}}{F_{\text{in}} c_{\text{in}} (t_{\text{pr}} + t_{\text{ads}})} \times 100\% \quad (1)$$

Where  $V_{\text{out}}$  is the product volume per cycle,  $c_{\text{out}}$  is the methane concentration in product,  $F_{\text{in}}$  is the flow rate of feed gas,  $c_{\text{in}}$  is the methane content in feed gas;  $t_{\text{pr}}$  and  $t_{\text{ads}}$  are the time for pressurization and adsorption, respectively. The adsorbent productivity is defined as the volume of feed gas processed per unit mass/volume of adsorbent per unit time

$$C_M = \frac{F_{\text{in}} (t_{\text{pr}} + t_{\text{ads}})}{t_{\text{tot}} m_{\text{AC}}} \quad (2)$$

$$C_V = \frac{F_{\text{in}} (t_{\text{pr}} + t_{\text{ads}})}{t_{\text{tot}} V_{\text{AC}}} \quad (3)$$

where  $C_M$  and  $C_V$  are the adsorbent productivity per unit mass and unit volume, respectively;  $t_{\text{tot}}$  is the time for a cycle period,  $m_{\text{AC}}$  is the mass of adsorbent packed in column, and  $V_{\text{AC}}$  is the volume of adsorbent bed. To evaluate the effectiveness of the purging regeneration method, an index of regeneration cost  $C_{\text{reg}}$ , was defined as the ratio of purging gas used for decreasing the CO<sub>2</sub> content in tail gas down to 10% over the nitrogen available in a cycle

**Table 2. Composition of Testing Gases**

Mixture	CH <sub>4</sub> %	N <sub>2</sub> %	He %
He/CH <sub>4</sub> /N <sub>2</sub>	6.30	7.12	86.58
CH <sub>4</sub> /N <sub>2</sub>	17.62	82.38	—
CH <sub>4</sub> /N <sub>2</sub>	22.30	77.70	—
CH <sub>4</sub> /N <sub>2</sub>	32.06	67.94	—
CH <sub>4</sub> /N <sub>2</sub>	40.28	59.72	—
CH <sub>4</sub> /N <sub>2</sub>	51.33	48.67	—

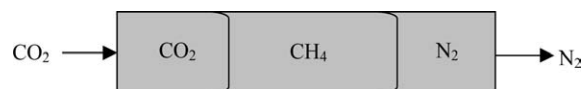


**Chart 2. The two concentration profiles along the adsorption bed in step 3.**

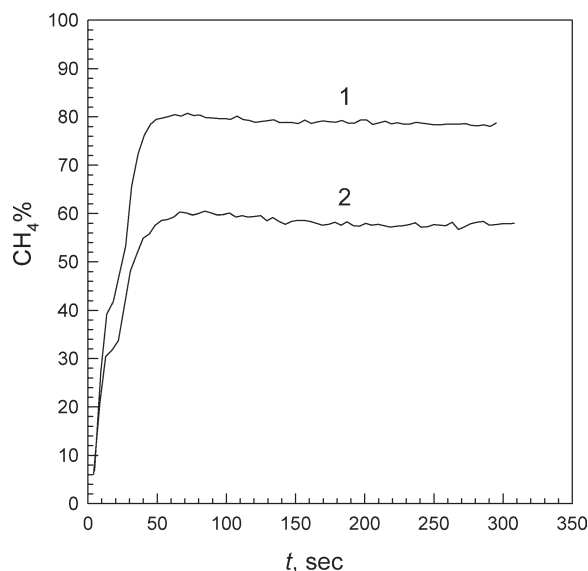


**Figure 6. Methane concentration in the desorbed gas (adsorption pressure = 0.4 MPa, and bed regeneration by evacuation).**

(1) Releasing pressure cocurrently, and (2) releasing pressure counter-currently.

$$C_{\text{reg}} = \frac{F_{\text{pg}} t_{\text{pg}}^{0.1}}{F_{\text{in}} c_N (t_{\text{pr}} + t_{\text{ads}})} \quad (4)$$

Where  $F_{\text{pg}}$  is the flow rate of purging gas;  $t_{\text{pg}}^{0.1}$  is the purging time required for decreasing the  $\text{CO}_2$  content in tail gas down to 10%;  $c_N$  is the concentration of nitrogen in feed gas. When the sorption bed was regenerated by evacuation, the degree of regeneration  $D_{\text{reg}}$ , was defined as the ratio of breakthrough times

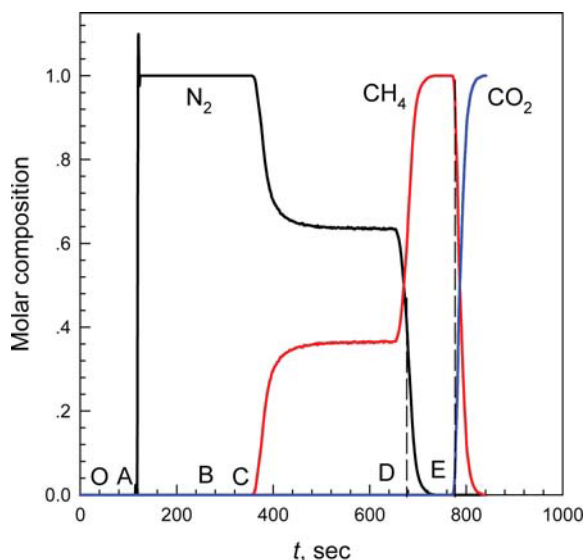


**Figure 7. Composition variation of the effluent stream for  $\text{CO}_2$  displacement at adsorption pressure 0.4 MPa.**

[Color figure can be viewed in the online issue, which is available at [wileyonlinelibrary.com](http://wileyonlinelibrary.com).]

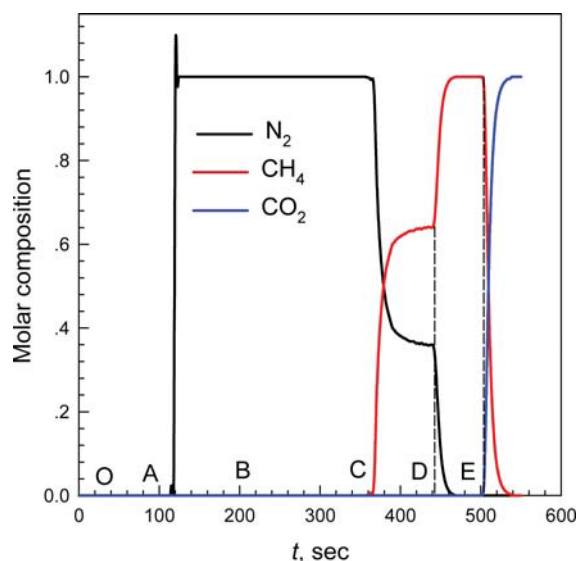


**Figure 8. Composition variation of the effluent stream for  $\text{CO}_2$  displacement at ambient pressure 0.1 MPa.**

[Color figure can be viewed in the online issue, which is available at [wileyonlinelibrary.com](http://wileyonlinelibrary.com).]

$$D_{\text{reg}} = \frac{t_{\text{re}}}{t_1} \quad (5)$$

Where  $t_{\text{re}}$  is the breakthrough time after regeneration, and  $t_1$  is the breakthrough time when a gas mixture passes through a fresh sorption bed.

## Results and Discussion

### Enrichment without $\text{CO}_2$ displacement

Methane as the stronger adsorbed component is concentrated in adsorbent, and can merely be a column-bottom product on

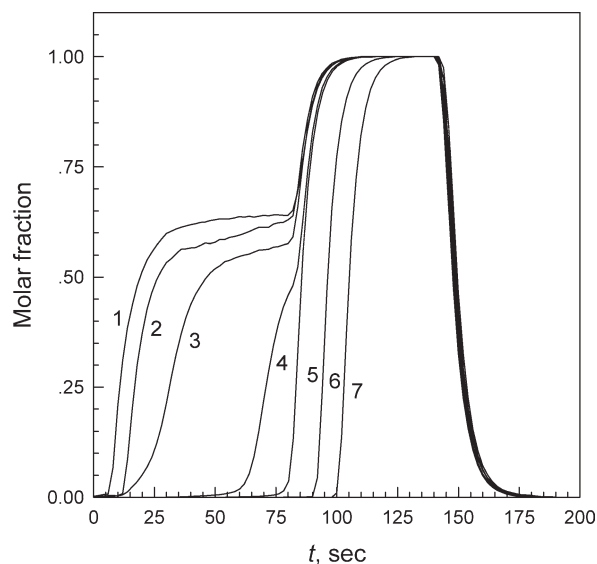


**Figure 9. Effect of adsorption time on displacement consequence (displacement at 0.1 MPa).**

(1)  $t_{\text{ads}} = 360$  s, (2)  $t_{\text{ads}} = 240$  s, (3)  $t_{\text{ads}} = 180$  s, (4)  $t_{\text{ads}} = 150$  s, (5)  $t_{\text{ads}} = 140$  s, (6)  $t_{\text{ads}} = 120$  s, and (7)  $t_{\text{ads}} = 100$  s.



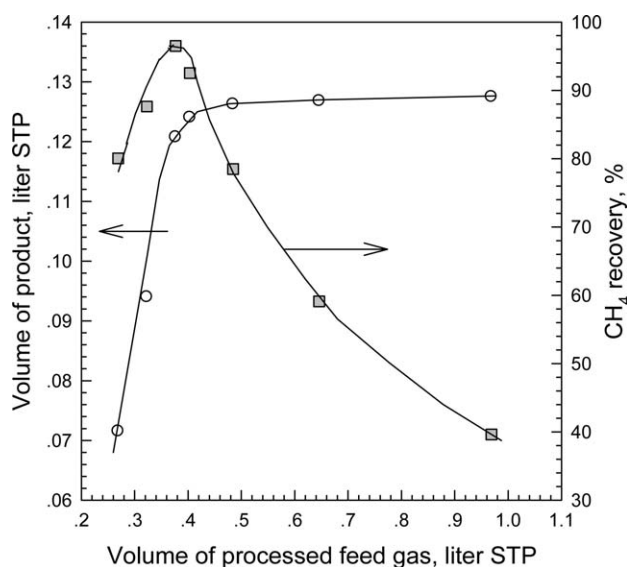


**Figure 10. Effect of processed feed gas per cycle on product quantity and methane recovery (CO<sub>2</sub> displacement at 0.1 MPa).**

releasing bed pressure and/or on the following evacuation without CO<sub>2</sub> displacement. However, the product concentration cannot be higher than 80% as shown in Figure 6 for the enrichment of feed gas containing 32.06% CH<sub>4</sub>.

#### Enrichment with CO<sub>2</sub> displacement

In the proposed PSA cycle, the step of adsorption was followed by a step of CO<sub>2</sub> displacement. Because CO<sub>2</sub> is more strongly adsorbed than CH<sub>4</sub> on activated carbon, the adsorbed CH<sub>4</sub> was displaced by the incoming CO<sub>2</sub> and enriched in gas phase. Figure 7 illustrates the displacement procedure when it takes place at the pressure of adsorption. The figure ordinate is the molar composition of the effluent stream. The OA period corresponded to the pressurization step, and the bed pressure increased from 0.1 to 0.4 MPa without any effluent stream. The AB period corresponded to the adsorption step, and nitrogen broke through the bed when the feed gas continued to enter at pressure 0.4 MPa. The feeding stream switched from feed gas to CO<sub>2</sub> at point B, and the displacement step began. Nitrogen was still the “column-top” product until point C, where the methane profile front broke through the bed. However, the tail of the nitrogen profile had not left the bed yet, and a mixture of N<sub>2</sub> and CH<sub>4</sub> flew out of the bed until point D, where the tail of the nitrogen profile left and a concentrated methane stream obtained at column-top. The feeding CO<sub>2</sub> was shut off at point E, where the profile front of CO<sub>2</sub> had just reached the bed top, and the fourth

step began. The concentrated CO<sub>2</sub> stream after point E was recorded during bed regeneration. A plug-flow regime was certainly provided for the displacement procedure. Figure 8 shows the same procedure for the CO<sub>2</sub> displacement occurring at ambient pressure. Comparing the two figures, it is observed that the time for the CD period considerably decreased if the displacement occurs at ambient pressure; therefore, less mixture of N<sub>2</sub> and CH<sub>4</sub> was produced. Due to pressure release, the methane content in the mixture for period CD becomes higher than that shown in Figure 7.

#### Selection of adsorption time

The CD period in either Figures 7 or 8 corresponds to a mixture of CH<sub>4</sub> and N<sub>2</sub> coexisting in the effluent stream. Obviously, the shorter is the CD period, the better is the cycle productivity, and the higher is the product concentration. The CD period can be compressed to the utmost by controlling the time allocated for adsorption. The coexisting gas mixture decreased, and finally disappeared with the decrease of adsorption time from 360 s to 140 s as shown in Figure 9 for the displacement occurring at ambient pressure as an example. With disappearance of the CD period, an effluent stream of high-methane content was obtained. Because the amount of feed-gas processed per cycle is largely determined by the time of adsorption, there is optimal process productivity correspondingly, at which both product volume and methane recovery show the largest value as shown in Figure 10. The optimal adsorption time is 140 s and the corresponding optimal quantity of feed gas processed per cycle is 0.377 L STP for CO<sub>2</sub> displacement at 0.1 MPa, and that for CO<sub>2</sub> displacement at 0.4 MPa is 210 s and 0.565 L STP, respectively. However, the productivity per unit mass of adsorbent is larger if the displacement occurred at 0.1 MPa as shown in Table 3. The composition of effluent stream during a cycle at the optimal operation regime is shown in Figure 11 for the displacement at 0.1 MPa as an example. OA marks the pressurization period, and AB the adsorption period. The bed pressure was released to ambient at point B, and CO<sub>2</sub> displacement took place till point E. The “top product” was N<sub>2</sub> for period BD, and it switched to CH<sub>4</sub>-enriched gas for period DE. The period CD disappeared and no mixture was produced.

#### Relationship between product concentration and methane recovery

The relationship between product concentration and methane recovery was affected by methane content in the feed gas and the mode of CO<sub>2</sub> displacement. When the displacement occurred at the adsorption pressure, methane recovery declined initially moderately following the increase of product concentration, and the decline accelerated at high concentrations. However, if the CO<sub>2</sub> displacement occurred at ambient pressure, methane

**Table 3. Effect of Methane Content in Feed Gas on Adsorption Time and Process Productivity**

Run	$c_{in}$ , %	Displacement at 0.4 MPa		Displacement at 0.1 MPa	
		$t_{ads}$ , sec	$C_M$ , l/Kg.h (STP)	$t_{ads}$ , sec	$C_M$ , l/Kg.h (STP)
1	51.33	200	262.6	130	270.7
2	40.28	200	275.5	130	289.1
3	32.06	210	300.0	140	320.7
4	22.30	210	306.7	140	327.8
5	17.62	210	314.1	140	335.8

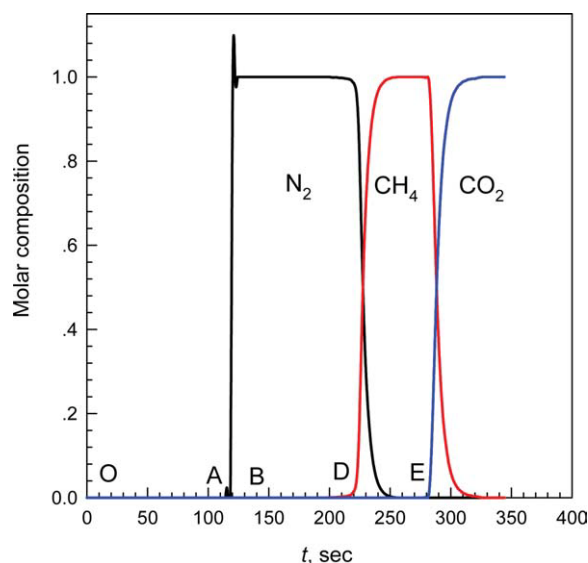


**Figure 11.** Effluent stream composition at the optimal operation regime ( $\text{CO}_2$  displacement at 0.1 MPa).

[Color figure can be viewed in the online issue, which is available at [wileyonlinelibrary.com](http://wileyonlinelibrary.com).]

recovery maintained a high level until the product concentration reached to an upper limit, and then the recovery fell down to the bottom as shown in Figures 12 and 13 for the two modes of  $\text{CO}_2$  displacement.

#### Effect of feed-gas concentration on enrichment

Methane content in the drainage gas of coal mining is generally 20–45%. Five compositions of feed gas were tested in this study, and the methane content ranges in 17.62–

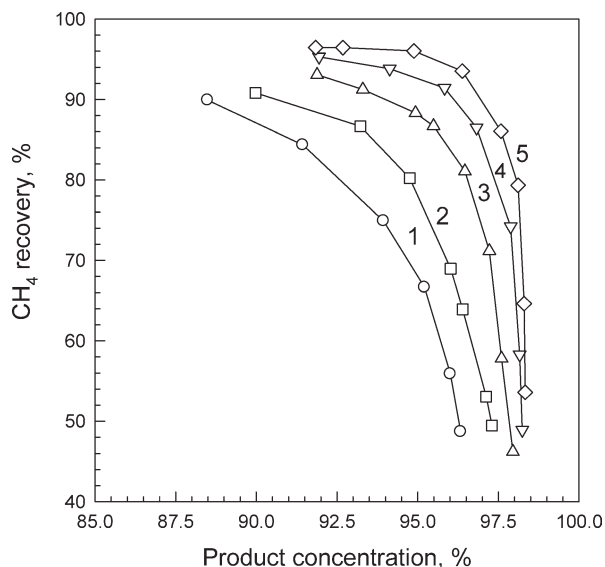


**Figure 12.** Product concentration and methane recovery for  $\text{CO}_2$  displacement at 0.4 MPa with feed-gas concentration of (1) 17.62%, (2) 22.30%, (3) 32.06%, (4) 40.28, and (5) 51.33%.

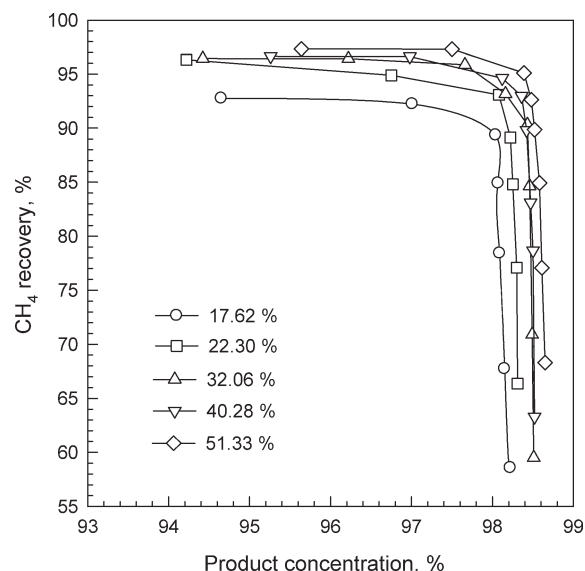


**Figure 13.** Product concentration and methane recovery for  $\text{CO}_2$  displacement at 0.1 MPa with different feed-gas concentrations.

51.33% as shown in Table 2. As shown in Figures 12 and 13, the methane content in feed gas showed remarkable effect on the reachable product concentration and methane recovery. Higher feed-gas concentration reaches higher product concentration and higher methane recovery; however, a product containing more than 90%  $\text{CH}_4$  was obtained with recovery higher than 98% even for a feed gas with low-methane concentration (17.62%) as shown in Figure 13. In addition, the optimal adsorption time also varies with feed-gas concentration as shown in Table 3. Shorter adsorption time applied for the feed gas of higher methane content, which resulted in less quantity of feed gas processed per cycle, and less adsorbent productivity.

#### Studies on regeneration

The regeneration performance of adsorbent is very important for a PSA process since it greatly affects the operation cost and the productivity of process. Two regeneration methods were tested in experiments. One method was purging the  $\text{CO}_2$ -saturated sorption bed with a  $\text{N}_2$  stream counter-currently at ambient pressure; another method was to evacuate the bed when the bed pressure had been released. Variation of  $\text{CO}_2$  content in the tail gas is shown in Figure 14 for different purging rates. The purging time decreases as purging rate increases; however, the index of regeneration cost gradually increased as shown in Figure 15 for two modes of  $\text{CO}_2$  displacement. A trade-off between purging time and regeneration cost must be made, and a purging rate of  $200 \text{ cm}^3/\text{min}$  was selected for subsequent experiments. The  $C_{\text{reg}}$  for the displacement at ambient pressure is larger than that for the displacement at the adsorption pressure due to the large difference in adsorption time. For example, the adsorption time was 140 s for the displacement at ambient pressure, and that for the displacement at adsorption pressure was 210 s; however, the purging time was the same for the two displacement modes. The fact that  $C_{\text{reg}}$  is larger than unity means

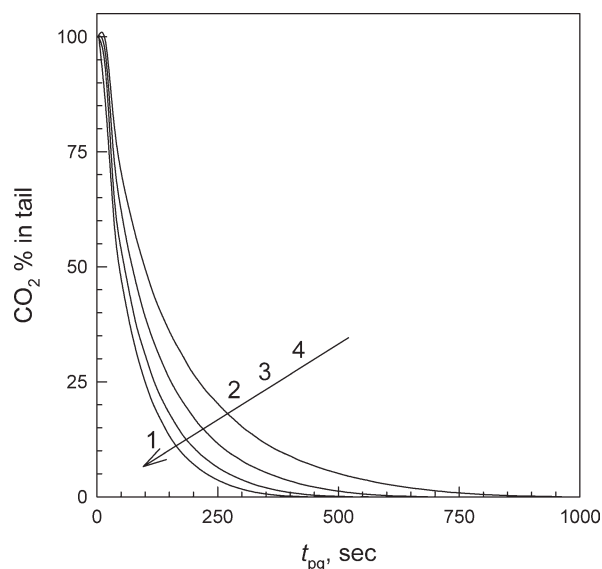


**Figure 14. CO<sub>2</sub> concentration in tail gas at different purging rates.**

(1) 250 cm<sup>3</sup>/min, (2) 200 cm<sup>3</sup>/min, (3) 150 cm<sup>3</sup>/min, and (4) 100 cm<sup>3</sup>/min.

the quantity of nitrogen produced in a cycle is not enough for purging; however, a separation between CO<sub>2</sub> and N<sub>2</sub> is required and both CO<sub>2</sub> and N<sub>2</sub> are reused. This separation may not contribute much to the total cost of CBM enrichment due to the limited volume of the CO<sub>2</sub>/N<sub>2</sub> mixture, and the fact that the separation between CO<sub>2</sub> and N<sub>2</sub> is easier than the separation between CH<sub>4</sub> and N<sub>2</sub>. In case that CO<sub>2</sub> is a component of CBM, the separation is no longer superfluous. The CO<sub>2</sub>-saturated sorption bed can also be regenerated by evacuation. For a given evacuation rate, the longer the

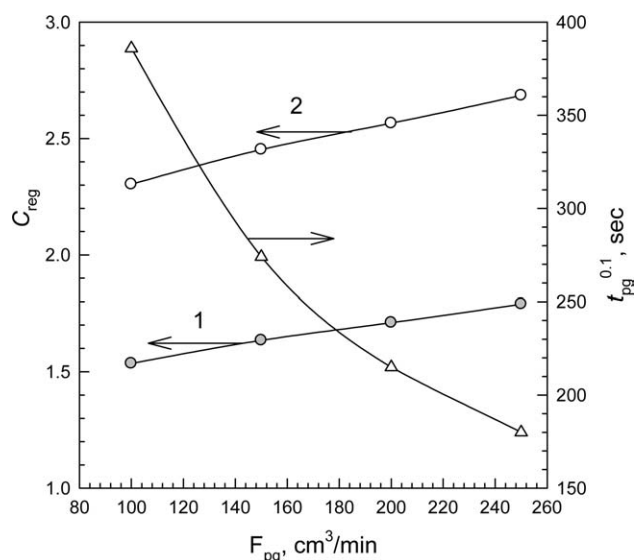


**Figure 15. Effect of purging rate on purging time and regeneration cost (evaluated for 10% of CO<sub>2</sub> content in tail gas).**

(1) CO<sub>2</sub> displacement at 0.4 MPa, and (2) CO<sub>2</sub> displacement at 0.1 MPa.

**Table 4. Effect of Evacuation Time on Regeneration Degree**

$t_{\text{vac}}$ , sec	$t_{\text{brk}}$ , sec	$D_{\text{reg}}$ , %
60	284	87.92
180	311	96.28
300	317	98.14
420	321	99.38
630	323	100
660	323	100

Note:  $t_{\text{vac}}$  is the time of evacuation, and  $t_{\text{brk}}$  is the breakthrough time after regeneration.

evacuation time the larger the regeneration degree. The dependence of regeneration degree on evacuation time is shown in Table 4. Apparently, the CO<sub>2</sub>-saturated bed can be fully regenerated by evacuation, and the desorbed CO<sub>2</sub> can be reused after compression.

### Test on consecutive cycling

Consecutive cycling was carried out at the optimal condition determined in previous PSA sections aiming to verify the stability of the proposed PSA process. The CO<sub>2</sub> displacement took place at ambient pressure, and both purging and evacuation methods were tested for bed regeneration. Product concentration and methane recovery are shown in Figure 16 for both regeneration methods. As shown in the figure, both regeneration methods result in almost the same process performance, and the process can be operated continuously.

### Comparison with literature

A comparison with other studies is made and summarized in Table 5, where the feed gas containing 32.06%CH<sub>4</sub> was taken as representative of this technology because this methane content is in the middle of the CH<sub>4</sub> content range tested. Although this study deals with the lowest feed concentration, the product concentration, methane recovery and adsorbent

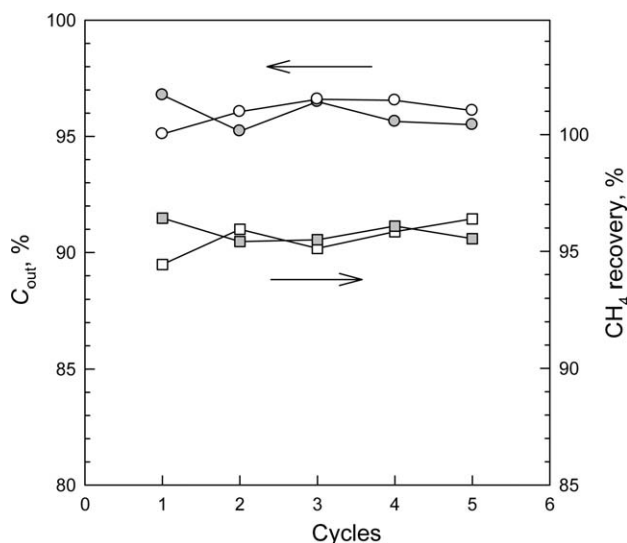


**Figure 16. Product concentration and methane recovery in consecutive cycles.**

White points (purging), gray points (evacuation), and CH<sub>4</sub> content in the feed gas is 32.06%.



**Table 5. Comparison of Enrichment Result with Literature**

Method	Adsorbent	CH <sub>4</sub> % of Feed	T, K	p, MPa	CH <sub>4</sub> % in product	CH <sub>4</sub> % Recovered	Productivity l/kg.h (STP)	P/F
Present	AC <sup>a</sup>	32.06	298	0.4	97.66	95.87	320.7	–
PSA <sup>11</sup>	AC	50	298	0.2	98.43	59.75	200	0.5
VPSA <sup>12</sup>	AC	55.2	278	0.3	96–98	86–91	–	1.8–2.1
PSA <sup>15</sup>	CMS <sup>b</sup>	50	298	0.2	79.2	48.5	–	–
PSA <sup>16</sup>	CMS	60	298	0.3	75.84	75.52	–	1.79
PSA <sup>25</sup>	ETS-4	85	295	0.7	97.2	53.2	–	–
	Clinop <sup>c</sup>				95.4	73.1		
	Mg-Clinop <sup>d</sup>				93.3	41.65		
PSA <sup>34</sup>	Solialite	85	298	0.12	96	74	106.8	–
LPSA <sup>35</sup>	CMS	60	301	0.25	86	52.6	–	–

Note: <sup>a</sup>Activated carbon; <sup>b</sup>Carbon molecular sieve; <sup>c</sup>Clinoptilolites; <sup>d</sup>Mg- Clinoptilolites.

productivity are at the top level. The excellent enrichment result must be attributed to the inclusion of CO<sub>2</sub> displacement into the PSA cycle.

$t_{\text{tot}}$  = time for a cycle period, s  
 $V_{\text{AC}}$  = volume of adsorbent bed, cm<sup>3</sup>  
 $V_{\text{out}}$  = product volume per cycle, cm<sup>3</sup>

## Conclusion

1. Inclusion of CO<sub>2</sub> displacement into a conventional PSA process succeeded to switch methane from column bottom to column top provided that the separation was based on equilibrium adsorption.

2. As a result of CO<sub>2</sub> displacement, a low-concentration feed gas (methane content 17.62%) was enriched to concentrated gas containing more than 90% CH<sub>4</sub> with methane recovery higher than 98%.

3. The CO<sub>2</sub> displacement at ambient pressure results in higher product concentration, higher methane recovery, and higher adsorbent productivity than the displacement occurring at the adsorption pressure.

4. Both purge with nitrogen and evacuation can fully regenerate the activated carbon saturated by CO<sub>2</sub>.

## Acknowledgments

Support of the National Natural Science Foundation of China (#20336020 and #91010005) and Basic Research of Tianjin Municipal Science and Technology Commission (07JCYBJC00800) is gratefully acknowledged.

## Notation

$C_M$  = adsorbent productivity per gram, cm<sup>3</sup> (STP)/g. min  
 $C_{\text{reg}}$  = index of regeneration cost  
 $C_V$  = adsorbent productivity per unit volume, l/min  
 $c_{\text{in}}$  = methane concentration in feed gas, %  
 $c_N$  = concentration of N<sub>2</sub> in feed gas, %  
 $c_{\text{out}}$  = methane concentration in product, %  
 $D_{\text{reg}}$  = degree of regeneration, %  
 $F_{\text{in}}$  = flow rate of feed gas, cm<sup>3</sup>/min  
 $F_{\text{pg}}$  = flow rate of purging gas, cm<sup>3</sup>/min  
 $m_{\text{AC}}$  = mass of adsorbent packed in column, g  
 $n$  = adsorbed amount, mmol/g  
 $P/F$  = purging ratio, defined as the ratio of the column-top component contained in purging stream to that contained in feed stream for a cycle  
 $p$  = adsorption pressure, MPa  
 $p_s$  = saturation pressure, MPa  
 $T$  = temperature, K  
 $t_1$  = time for breaking through a fresh sorption bed, s  
 $t_{\text{ads}}$  = adsorption time, s  
 $t_{\text{pg}}^{0.1}$  = purging time required for decreasing the CO<sub>2</sub> content in tail gas down to 10%, s  
 $t_{\text{pr}}$  = time for pressurization, s  
 $t_{\text{re}}$  = breakthrough time after regeneration, s

## Literature Cited

- Q. Jiang. Report on China Coal Bed Methane Industry for 2010–2015. <http://www.ocn.com.cn/reports/2006131meiceng.htm>, 2010.
- Flores RM. Coal-bed methane: from hazard to resource. *Int J Coal Geology*. 1998;35:3–26.
- Engelhard Corp. Adsorption processes for natural gas treatment, a technology update. [www.engelhard.com](http://www.engelhard.com); 2005.
- Ruthven DM. Past progress and future challenges in adsorption research. *Ind Eng Chem Res*. 2000;39:2127–2131.
- Yang RT. *Gas Separation by Adsorption Process*. Boston, MA: Butterworths; 1987:50–101.
- Cecopieri-Gomez ML, Palacios-Alquisira J, Dominguez JM. On the limits of gas separation in CO<sub>2</sub>/CH<sub>4</sub>, N<sub>2</sub>/CH<sub>4</sub> and CO<sub>2</sub>/N<sub>2</sub> binary mixtures using polyimide membranes. *J Membrane Sci*. 2007;293:53–65.
- Lokhandwala KA, Pinnau I, He ZhJ, Amo KD, DaCosta AR, Wijmans JG, Baker RW. Membrane separation of nitrogen from natural gas: A case study from membrane synthesis to commercial deployment. *J Membr Sci*. 2010;346:27–279.
- Ruthven DM. *Principles of Adsorption and Adsorption Process*. New York: John Wiley & Sons; 1984:29–85.
- Ruthven DM, Farooq S, Knaebel KS. *Pressure Swing Adsorption*. New York: VCH Publisher; 1994:1–288.
- Sheik MA, Hassan MM, Loughlin KF. Adsorption equilibria and rate parameters for nitrogen and methane on maxsorb activates carbon. *Gas Sep Purif*. 1996;10:161–168.
- Baksh MSA, Kapoor A, Yang RT. A new composite sorbent for methane-nitrogen separation by adsorption. *Sep Sci Technol*. 1990;25:845–868.
- Olajossy A, Gawdzik A, Budner Z, Dula J. Methane separation from coal mine methane gas by vacuum pressure swing adsorption. *Chem Eng Res Des*. 2003;81:474–482.
- Warmuzinski K, Sodzawiczny W. Effect of adsorption pressure on methane purity during PSA separations of CH<sub>4</sub>/N<sub>2</sub> mixture. *Chem Eng Process*. 1999;8:55–60.
- Ruthven DM, Xu Z, Farooq S. Sorption kinetics in PSA systems. *Gas Sep Pur*. 1993;7:75–81.
- Ackley MW, Yang RT. Kinetic separation by pressure swing adsorption: method of characteristics model. *AIChE J*. 1990;36:1229–1238.
- Fatehi AI, Loughlin KF, Hassan MM. Separation of methane-nitrogen mixtures by pressure swing using a carbon molecular sieve. *Gas Sep Pur*. 1995;9:199–204.
- Simone C, Carlos AG, Rodrigues AE. Separation of methane and nitrogen by adsorption on carbon molecular sieve. *Sep Sci Technol*. 2005;40:2721–2743.
- Tezel F, Apolonatos HG. Chromatographic study of adsorption for N<sub>2</sub>, CO and CH<sub>4</sub> in molecular sieve zeolites. *Gas Sep Pur*. 1993;7:11–17.
- Ruthven DM, Kumar R. A chromatographic study of the diffusion of N<sub>2</sub>, CH<sub>4</sub> and binary CH<sub>4</sub>-N<sub>2</sub> mixtures in 4A molecular sieve. *Can J Chem Eng*. 1979;57:342–348.

20. Mohr RJ, Vorkapic D, Rao MB, Sircar S. Pure and binary gas adsorption equilibria and kinetics of methane and nitrogen on 4a zeolite by isotope exchange technique. *Adsorption*. 1999;145–158.
21. Habgood HW. The kinetics of molecular sieve action sorption of nitrogen-methane mixtures by linder molecular sieve 4A. *Can J Chem*. 1958;36(10):1384–1397.
22. Ackley MW, Yang RT. Diffusion in ion-exchanged clinoptilolites. *AIChE J*. 1991;37:1645–1656.
23. Ackley MW, Yang RT. Clinoptilolite: Untapped potential for kinetic gas separations. *Zeolites*. 1992;12:780–788.
24. Ackley MW, Yang RT. Adsorption characteristics of high-exchange clinoptilolites. *Ind Eng Chem Res*. 1991;30:2523–2530.
25. Jayaraman A, Arturo J, Yang RT, Chinn D, Munson CL, Mohr DH. Clinoptilolites for nitrogen/methane separation. *Chem Eng Sci*. 2004;59: 2407–2417.
26. Jayaraman A, Arturo J, Yang RT, Chinn D, Munson CL, Mohr DH. Tailored clinoptilolites for nitrogen/methane separation. *Ind Eng Chem Res*. 2005;44:5184–5192.
27. Harlick PJE, Tezel FH. Adsorption of carbon dioxide, methane and nitrogen: pure and binary mixture adsorption for ZSM-5 with SiO<sub>2</sub>/Al<sub>2</sub>O<sub>3</sub> ratio of 280. *Sep Pur Technol*. 2003;33:199–210.
28. Maple MJ, Williams CD. Separating nitrogen/methane on zeolite-like molecular sieves. *Micro Meso Mater*. 2008;111:627–631.
29. Kouvelos E, Kesore K, Steriotis T, Grigoropoulou H, Bouloubasi D, Theophilou N, Tzintzos S, Kanelopoulos N. High pressure N<sub>2</sub>/CH<sub>4</sub> adsorption measurement in clinoptilolites. *Micro Meso Mater*. 2007;99: 106–111.
30. Li PY, Tezel FH. Adsorption separation of N<sub>2</sub>, O<sub>2</sub>, CO<sub>2</sub> and CH<sub>4</sub> gases by  $\beta$ -zeolite. *Micro Meso Mater*. 2007;98:94–101.
31. Li PY, Tezel FH. Pure and Binary Adsorption of methane and nitrogen by silicalite. *J Chem Eng Data*. 2009;54:8–15.
32. Lastoskie C, Gubbins KE, Quirke N. Pore size heterogeneity and the carbon slit pore: A density functional theory model. *Langmuir*. 1993;9:2693–2702.
33. Zhou L, Zhou YP, Li M, Chen P, Wang Y. Experimental and modeling study of the adsorption of supercritical methane on a high surface carbon. *Langmuir*. 2000;16:5955–5959.
34. Delgado JA, Uguina MA, Sotelo JL, Ruiz B. Modelling of the fixed-bed adsorption of methane/nitrogen mixtures on silicalite pellets. *Sep Pur Technol*. 2006;50:192–203.
35. Cavenati S, Grande CA, Rodrigues AE. Separation of CH<sub>4</sub>/CO<sub>2</sub>/N<sub>2</sub> mixtures by layered pressure swing adsorption for upgrade of natural gas. *Chem Eng Sci*. 2006;61:3893–3906.

Manuscript received Feb. 21, 2010, and revision received Apr. 17, 2010.